

Yellow Luminescence of Gallium Nitride Generated by Carbon Defect Complexes

D. O. Demchenko, I. C. Diallo, and M. A. Reshchikov

Department of Physics, Virginia Commonwealth University, Richmond, Virginia 23284, USA

(Received 11 September 2012; published 21 February 2013)

We demonstrate that yellow luminescence often observed in both carbon-doped and pristine GaN is the result of electronic transitions via the C_N-O_N complex. In contrast to common isolated defects, the C_N-O_N complex is energetically favorable, and its calculated optical properties, such as absorption and emission energies, a zero phonon line, and the thermodynamic transition level, all show excellent agreement with measured luminescence data. Thus, by combining hybrid density functional theory and experimental measurements, we propose a solution to a long-standing problem of the GaN yellow luminescence.

DOI: [10.1103/PhysRevLett.110.087404](https://doi.org/10.1103/PhysRevLett.110.087404)

PACS numbers: 78.55.Cr, 61.72.uj, 71.15.Mb, 71.55.Eg

Technological advancements in GaN doping have made it a suitable material for applications in recently developed blue and green light-emitting diodes [1], the blue-emitting GaN-based lasers [2,3], and solar cells [4]. Understanding the optical and electronic properties of defects in GaN is of great importance for evaluating the degree to which they affect the devices' performance. The most notoriously controversial defect-induced optical transition in GaN is centered around 2.2–2.3 eV and is often referred to as the yellow luminescence (YL) [5–7]. This YL band is usually observed in *n*-type GaN [5,8], both for undoped samples [9] and samples containing carbon impurities [10–12]. Nevertheless, the microscopic origin of the YL band has been debated for almost 30 years, and the exact attribution of the YL band to specific defects in GaN has been unclear. Early works attributed the YL band to the formation of the $V_{Ga}-C_{Ga}$ complex [6]. With the development of density functional theory, it has been suggested that Ga vacancies, V_{Ga} , both isolated and bound into a complex with oxygen donors, O_N , (and possibly silicon donors, Si_{Ga}) are responsible for the observed YL [13,14]. These theoretical results have found some experimental support where positron annihilation experiments showed apparent correlation of the YL intensity with the concentration of Ga vacancies [15]. On the other hand, experimental findings have also indicated that lattice defects alone do not cause YL, rather H, C, and O, possibly bound into complexes, produce the observed YL band [12]. Most recently it has been suggested that carbon substituting for nitrogen C_N creates a deep acceptor in GaN, which may be responsible for the YL band [16].

In this Letter, we demonstrate that the C_N-O_N complex is responsible for the observed carbon related YL in GaN. Using hybrid density functional theory and experimental photoluminescence (PL) measurements, we show that the calculated emission and absorption energies, zero phonon line, and thermodynamic transition level for the C_N-O_N complex are all in excellent agreement with the PL data. Furthermore, the formation energy of the carbon bound into the C_N-O_N complex is significantly lower than that of

any other carbon defect. A systematic study has been performed in order to eliminate possible alternative explanations, including isolated defects and complexes, thus offering a solution to the YL problem.

Figure 1 shows the spectral dependence (inset) and the temperature dependence of the PL intensity for the YL band in GaN. The YL band has an abrupt onset at 2.6 eV (which can be identified as the zero-phonon energy), a maximum at 2.20 eV and the full-width at half maximum of 410 meV at 15 K. From the fit of the temperature dependence of the YL intensity (Fig. 1) we have determined the activation energy (thermodynamic transition level) of $E_A = 850$ meV for the defect responsible for the YL band. The hole-capture coefficient, C_{pA} , obtained from this fit (6×10^{-7} cm³/s) is close to the values reported in the literature [5], and other parameters are very similar to the parameters of the YL band in C-doped GaN [6]. We observed a moderate shift to higher energies

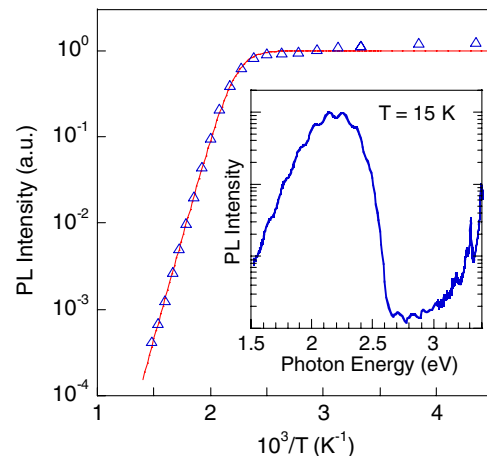


FIG. 1 (color online). Temperature dependence of the YL band intensity. Excitation power density is 0.3 mW/cm². The line is a fit with Eq. (6) from Ref. [5] with the following parameters: $\tau_R = 3.7 \times 10^{-4}$ s (determined from the time-resolved PL), $E_A = 850$ meV, $C_{pA} = 6 \times 10^{-7}$ cm³/s. The inset shows the PL spectrum at 15 K.

by only 8 ± 2 meV with increasing excitation power density from 10^{-6} to 0.1 W/cm². This shift is commonly explained by the donor-acceptor-pair (DAP) type transition, where an electron bound to a shallow donor recombines with a hole bound to a deep acceptor. Because of the DAP interpretation, most defects suggested in the literature as sources of YL in GaN have been deep acceptors. However, as we show below, this is not necessarily the case. The sample used to obtain these results was grown by metalorganic chemical vapor deposition, and contained Si, C, and O atoms with concentrations of 3×10^{16} , 4×10^{16} , and 5×10^{16} cm⁻³, respectively [17]. However, the concentration of the defects responsible for the YL band in this sample has been estimated to be 3.3×10^{15} cm⁻³ [18]. Therefore, the concentration of defects responsible for the YL band is much lower than the concentrations of elemental point defects, suggesting that defect complexes, which have concentrations lower than that of the elemental defects, can explain this discrepancy.

Our theoretical approach is based on the hybrid functional method which in recent years has become a preferred approach for the analysis of defects and their properties in semiconductors [19]. It offers a practical compromise between the semilocal or local approximations to the density functional theory [20] and the computationally demanding many-body methods (*GW*) [21,22]. Our calculations are based on the Heyd-Scuseria-Ernzerhof (HSE) hybrid functional [23] as implemented in the VASP program [24], with the projector augmented wave method [25,26]. In an exchange tuned hybrid functional calculation of defects in semiconductors, the semilocal density exchange-correlation part of the density functional is mixed with a Fock-type exchange part in a ratio adjusted to match the band gap of the host material. Compared to semilocal functionals, this also improves the host lattice properties [27], which is important to capture the defect relaxation properties. We use the HSE hybrid functional with the fraction of exact exchange of 0.31, and the screening parameter of 0.2 \AA^{-1} . These parameters accurately reproduce both the band gap and the lattice properties of bulk GaN [28]. The resulting band gap of 3.49 eV is in good agreement with the low-temperature experimental value of 3.50 eV [29]. We used the value of the band gap renormalized by zero-point motion [30] to incorporate these effects into the gap fitting. Computed relaxed lattice parameters for wurtzite GaN ($a = 3.210 \text{ \AA}$, $c = 5.198 \text{ \AA}$, and $u = 0.377$) also agree with experimental values ($a = 3.189 \text{ \AA}$, $c = 5.185 \text{ \AA}$) [31]. The 128 atom supercells were used with atomic structures relaxed using HSE hybrid functional calculations to yield forces of 0.05 eV/\AA or less. The plane-wave basis sets with 400 eV cutoff at the Γ point were used in all electronic structure calculations. Spin-polarized calculations were performed in all cases. Systematic tests were performed in order to identify and evaluate the sources of error, and the influence of any of

these parameters on the defect thermodynamic and optical transition levels.

The defect formation energy E_f determines the probability of a particular defect configuration to be realized. It is defined [20] $E_f = E_{\text{tot}}^{\text{def}} - E_{\text{tot}}^{\text{bulk}} - \sum_i \Delta n_i \mu_i + qE_F + \Delta V + \Delta E_{\text{MP}}$, as the total energy difference of the supercell with the defect and the bulk supercell, minus their difference in the chemical potentials μ_i for the number of atoms difference Δn_i in the two cells, adding the energy cost of charging the defect qE_F , assuming the exchange of electrons with the Fermi level E_F . The two remaining terms correct for the electrostatic errors of two different origins. The potential alignment ΔV arises from dropping the diverging $\mathbf{G} = 0$ term in the Fourier energy expansion in a charged supercell [32]. This term is usually small (0.05 to 0.15 eV) and proportional to the defect formal charge q . The last term is the spurious electrostatic interaction correction for charged defects, following Makov and Payne [33,34]. Here the Madelung energy was used along with the 3rd order corrections analyzed in detail by Lany *et al.* [35]. Both terms scale as q^2 and depend on the supercell geometry. The Madelung energy for the 128 atom GaN $\pm 1e$ charged cell is ~ 0.20 eV, while the 3rd order term is ~ -0.073 eV. Following Ref. [36] we also applied Madelung corrections to neutral impurities where electrons (holes) occupy the conduction (valence) band, i.e., forming a charged ion in delocalized compensating charge density.

For the 128 atom cells used in this work, the use of the Γ point only rather than a k -point mesh was found to cause negligible errors. The total energy errors between the Γ point and the 222 k point either Monkhorst-Pack or Γ -centered mesh did not exceed 0.05 eV. A more significant source of error was found to be the plane-wave energy cutoff. In the literature for the typical HSE calculations of the defects in supercells, it is often set to 300 eV [16,28]. However, formation energies computed with a 400 eV energy cutoff were found to differ by about 0.1–0.2 eV from those of 300 eV. This error is not the same for different charge states of a given defect configuration, and therefore does not cancel out in optical transition calculations.

The remaining error related to the size of the cell includes several different error sources, i.e., elastic interactions and errors related to the supercell band structure. For example, between the 72 and 128 atom cells, the error in formation energy reaches 0.2 eV for isolated defects and up to 0.55 eV for some of the complexes. We tested hybrid functional calculations for supercells containing up to 300 atoms, and found that this error is reduced to about 0.15–0.2 eV for complexes and about 0.05 eV for isolated defects when using 128 atom cells. In some cases, this error can be estimated as the energy difference between the impurity band center of mass and the Γ -point eigenvalue [36]. We estimated these errors using generalized gradient approximation for supercell sizes ranging from 128 to 572

atoms, and found them to be 0.1 to 0.2 eV. These values are very similar for different charge states of the same defect, leading to error cancellation in the computed transition energies.

Formation energies of defect complexes.—The formation energies of different carbon defect configurations are presented in Figure 2, where in Ga-rich and Ga-poor growth conditions, Ga and N chemical potentials are separated by the GaN formation enthalpy, computed to be $\Delta H_{\text{GaN}} = -1.25$ eV. The only carbon-related defect complex that is found to be energetically favorable is the $\text{C}_\text{N}\text{-O}_\text{N}$ complex. For *n*-type GaN, its formation energy is more than 2.5 eV lower than that of the isolated C_N . The binding energy of this complex is 0.32 eV in both Ga-rich and Ga-poor conditions. However, in Ga-poor conditions the isolated oxygen donor has formation energy 1.4 eV lower than that of the complex, implying that in these conditions, complex concentrations will be low compared to those of the isolated impurities. In Ga-rich conditions, the complex formation energy is almost the same as that of O_N and ~ 2.6 eV lower than that of the C_N ; thus, the complex concentrations are expected to be large. The $\text{C}_\text{N}\text{-O}_\text{N}$ complex is a deep donor, with a 0/+ thermodynamic transition level at 0.75 eV above the valence band maximum (VBM), and a deeper +/2+ level at 0.14 eV above the VBM.

It has been suggested that Ga vacancy complexes could be responsible for the YL [6,13,14]. However, the PL band produced by the $\text{V}_{\text{Ga}}\text{-O}_\text{N}$ complex is computed here to be infrared, with a maximum at 1.42 eV. The $\text{V}_{\text{Ga}}\text{-C}_{\text{Ga}}$ complex is unlikely to form, due to a high formation energy (~ 9.2 eV in *n*-type GaN), leading to a negative binding energy. The donor-acceptor complex $\text{C}_\text{N}\text{-C}_{\text{Ga}}$ is also found here to have a high formation energy, 5.32 eV

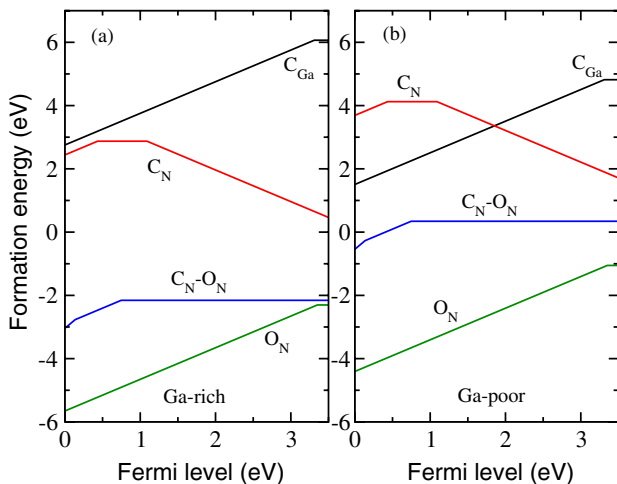


FIG. 2 (color online). Defect formation energies as a function of the Fermi energy in Ga-rich and Ga-poor growth conditions. Defect thermodynamic transition levels in the GaN band gap correspond to the intersections of different slopes (charge states) of each line.

for *n*-type GaN, regardless of the growth conditions and is unlikely to form.

In close agreement with previously published results, [16] we also find that the isolated C_N is a deep acceptor with a transition energy of 1.09 eV. We also find a deep +/0 transition level at 0.43 eV above the VBM. A substitutional C_{Ga} donor was also found to have a relatively high formation energy, in both Ga-rich and Ga-poor conditions, with the shallow donor level at 0.18 eV below the conduction band minimum (CBM). The shallow donor O_N is found to have a thermodynamic transition level 0.14 eV below the CBM. This defect has a negative formation energy, implying that all available oxygen atoms will readily form the substitutional donors. The negative formation energy stems from the fact that all gallium oxides have a much larger magnitude of the formation enthalpy compared to that of GaN [37]. For example, the computed enthalpy of formation for common Ga_2O_3 is -10.5 eV, compared to -1.25 eV for GaN.

Optical transitions.—The calculated optical transitions using configuration coordinate diagrams are presented in Fig. 3. Initially, the ground state of the $\text{C}_\text{N}\text{-O}_\text{N}$ complex in the *n*-type GaN is neutral. As a result of the optical excitation producing an electron-hole pair, the $\text{C}_\text{N}\text{-O}_\text{N}$ complex captures the hole which transfers the complex into a $(\text{C}_\text{N}\text{-O}_\text{N})^+$ charge state. The excitation energy for this transition is calculated to be 3.30 eV, which agrees with the experimental values of 3.19 [6] and 3.32 eV [38]. Losing the excess energy through the lattice relaxation, the $(\text{C}_\text{N}\text{-O}_\text{N})^+$ complex relaxes into the minimum energy structure of the excited state. Figure 3 also shows the computed electronic band structure in the Γ -*M* direction,

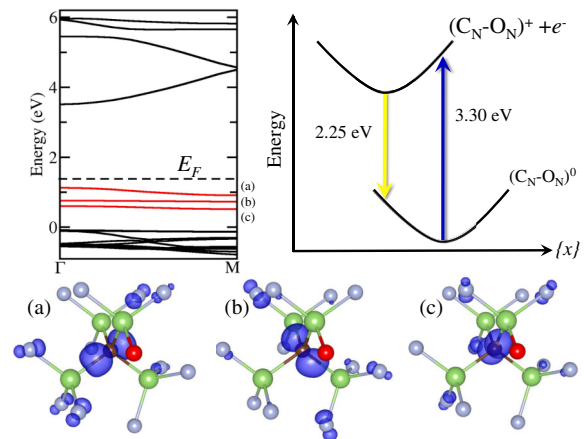


FIG. 3 (color online). Band structure of the $(\text{C}_\text{N}\text{-O}_\text{N})^0$ defect complex ground state. The three localized defect states are labeled (a), (b), and (c). The configuration coordinate diagram illustrates the absorption and emission energies. The charge densities of the three localized defect states are plotted at 15% of their maximum. Large green atoms are Ga, smaller light-gray atoms are N, the dark red atom is O (in the front), and the dark brown atom is C (in the center).

with the localized defect electronic levels [labeled (a), (b), and (c)] slightly broadened by the spurious interactions due to the use of periodic boundary conditions. The crystal structure used in these band structure calculations is fixed at the relaxed $(C_N-O_N)^+$ charged state, to represent the electronic structure related to the optical emission. The highest defect state will be occupied by the captured hole, allowing the subsequent radiative recombination of an electron in the CBM and the hole localized on the C_N-O_N complex [the localized charge density of the hole is also shown in Fig. 3(a)]. This emission energy for the maximum of the YL band is computed to be 2.25 eV. The subsequent $(C_N-O_N)^0$ lattice relaxation energy (Franck-Condon shift) is computed to be 0.48 eV, yielding the zero-phonon transition at 2.7 eV. As a result, the complex returns to its ground state $(C_N-O_N)^0$. The difference between the absorption and emission peaks (Stokes shift) is found to be 1.05 eV. These calculated results are in excellent agreement with our measurements, where the PL emission peak is found at 2.20 eV (Fig. 1), supporting our proposed YL source as the C_N-O_N complex. They also agree very well with configuration diagrams deduced from early experiments in Ref. [6].

Recently, Lyons *et al.* [16] have suggested that the YL band can be explained by the transitions to the C_N deep acceptor, obtaining 2.14 eV for the optical transition from the conduction band to the $C_N^{0/-}$ level. Using the 300 eV energy cutoff in our hybrid functional calculations, we reproduce these results. However, increasing the cutoff to 400 eV results in a deeper thermodynamic transition energy of 1.09 eV (0.9 eV in Ref. [16]), which does not agree well with a measured ionization energy of 0.85 eV for the YL-related acceptor obtained here and in early works on the subject [6]. This shift changes the calculated optical transition energy to a *red* optical transition with a maximum at 1.88 eV. The absorption band maximum also lowers and is found to be at 2.76 eV. Therefore, the calculated properties of the isolated C_N acceptor do not agree well with the experimental data for the carbon-related YL in GaN. On the other hand, the more energetically favorable C_N-O_N complex yields optical transitions in agreement with the measured PL spectrum (Figure 1).

The proposed explanation of the YL band by the C_N-O_N complex is also consistent with previously published experimental data. In particular, a blueshift of a PL band with increasing excitation intensity is commonly attributed to the DAP-type optical transitions involving a shallow donor and a deep acceptor [5]. However, the blueshift for a PL band can also be caused by transitions from shallow donors to a deep donor. For example, the presence of several types of shallow donors with different ionization energies would cause the same effect as the DAP with random distribution of pair separations. Moreover, the broadening of a shallow donor level due to the interaction of impurities is identical to the presence of several types of shallow donors.

Hitherto, the attribution of the YL-related defect to a deep acceptor rather than a deep donor historically always appeared more reasonable, because the capture of holes by negatively charged acceptors is more efficient than the capture by a neutral donor. Nevertheless, our estimates for deep-level defects in GaN indicate that the hole-capture efficiency for a neutral donor is only an order of magnitude lower than that for a negatively charged acceptor [39], which is sufficient to cause the observed YL.

In conclusion, we have demonstrated that the deep donor complex $(C_N-O_N)^0$ explains the microscopic mechanism of the YL in GaN. This complex has a low formation energy and therefore should be present in sufficient concentrations to cause the observed PL. Calculated optical transitions via the localized defect states of this complex are in excellent agreement with the measured PL data (experimental values are given in brackets): thermodynamic transition level of 0.75 eV (0.85 eV), absorption energy 3.30 eV (3.32 eV), emission energy 2.25 eV (2.20 eV), and zero phonon transition 2.70 eV (2.60 eV). This complex has not been proposed as a source of the yellow band in GaN, while all other defects previously suggested to be sources of this band exhibit high formation energies and would produce red or infrared PL. Thus, we resolve a 30-year-old problem of microscopic origin of yellow luminescence in GaN.

This work used the computational facilities of the VCU Center for High Performance Computing.

-
- [1] S. Nakamura, T. Mukai, and M. Senoh, *Appl. Phys. Lett.* **64**, 1687 (1994).
 - [2] S. Nakamura and G. Fasol, *The Blue Laser-Diode—GaN Based Light Emitters and Lasers* (Springer-Verlag, Berlin, 1997).
 - [3] F.A. Ponce and D.P. Bour, *Nature (London)* **386**, 351 (1997).
 - [4] R. Dahal, J. Li, K. Aryal, J. Y. Lin, and H. X. Jiang, *Appl. Phys. Lett.* **97**, 073115 (2010).
 - [5] M. A. Reshchikov and H. Morkoç, *J. Appl. Phys.* **97**, 061301 (2005).
 - [6] T. Ogino and M. Aoki, *Jpn. J. Appl. Phys.* **19**, 2395 (1980).
 - [7] T. Suski, P. Perlin, H. Teisseyre, M. Leszczyński, I. Grzegory, J. Jun, M. Boćkowski, S. Porowski, and T. D. Moustakas, *Appl. Phys. Lett.* **67**, 2188 (1995).
 - [8] M.O. Manasreh and H.X. Jiang, *Three-Nitride Semiconductors: Optical Properties* (CRC, New York, 2002), Vol. 1.
 - [9] E.R. Glaser, T.A. Kennedy, K. Doverspike, L.B. Rowland, D.K. Gaskill, J.A. Freitas Jr., M. Asif Khan, D.T. Olson, J.N. Kuznia, and D.K. Wickenden, *Phys. Rev. B* **51**, 13326 (1995).
 - [10] C.H. Seager, A.F. Wright, J. Yu, and W. Götz, *J. Appl. Phys.* **92**, 6553 (2002).
 - [11] A. Armstrong, A. R. Arehart, D. Green, U. K. Mishra, J. S. Speck, and S. A. Ringel, *J. Appl. Phys.* **98**, 053704 (2005).
 - [12] S. O. Kucheyev, M. Toth, M. R. Phillips, J. S. Williams, C. Jagadish, and G. Li, *J. Appl. Phys.* **91**, 5867 (2002).

- [13] J. Neugebauer and C. G. Van de Walle, *Appl. Phys. Lett.* **69**, 503 (1996).
- [14] T. Mattila and R. M. Nieminen, *Phys. Rev. B* **55**, 9571 (1997).
- [15] K. Saarinen, T. Laine, S. Kuisma, J. Nissilä, P. Hautojärvi, L. Dobrzynski, J. M. Baranowski, K. Pakula, R. Stepniewski, M. Wojdak, A. Wysmolek, T. Suski, M. Leszczynski, I. Grzegory, and S. Porowski, *Phys. Rev. Lett.* **79**, 3030 (1997).
- [16] J. L. Lyons, A. Janotti, and C. G. Van de Walle, *Appl. Phys. Lett.* **97**, 152108 (2010).
- [17] The GaN sample was grown and the secondary-ion mass-spectrometry data were provided by S.-P. Guo and D. W. Gotthold (EMCORE).
- [18] M. A. Reshchikov, *Appl. Phys. Lett.* **88**, 202104 (2006).
- [19] A. Alkauskas, P. Broqvist, and A. Pasquarello, *Phys. Rev. Lett.* **101**, 046405 (2008).
- [20] C. G. Van de Walle and J. Neugebauer, *J. Appl. Phys.* **95**, 3851 (2004).
- [21] S. Lany and A. Zunger, *Phys. Rev. B* **81**, 113201 (2010).
- [22] P. Rinke, A. Janotti, M. Scheffler, and C. G. Van de Walle, *Phys. Rev. Lett.* **102**, 026402 (2009).
- [23] J. Heyd, G. E. Scuseria, and M. Ernzerhof, *J. Chem. Phys.* **118**, 8207 (2003).
- [24] G. Kresse and J. Furthmüller, *Phys. Rev. B* **54**, 11169 (1996).
- [25] P. E. Blöchl, *Phys. Rev. B* **50**, 17953 (1994).
- [26] G. Kresse and D. Joubert, *Phys. Rev. B* **59**, 1758 (1999).
- [27] M. Marsman, J. Paier, A. Stroppa, and G. Kresse, *J. Phys. Condens. Matter* **20**, 064201 (2008).
- [28] J. L. Lyons, A. Janotti, and C. G. Van de Walle, *Phys. Rev. Lett.* **108**, 156403 (2012).
- [29] R. Dingle, D. D. Sell, S. E. Stokowski, and M. Ilegems, *Phys. Rev. B* **4**, 1211 (1971); B. Monemar, *Phys. Rev. B* **10**, 676 (1974).
- [30] F. J. Manjon, M. A. Hernandez-Fenollosa, B. Mari, S. F. Li, C. D. Poweleit, A. Bell, J. Menendez, and M. Cardona, *Eur. Phys. J. B* **40**, 453 (2004).
- [31] H. Morkoç, *Handbook of Nitride Semiconductors and Devices* (Wiley, New York, 2008), Vols. 1–3.
- [32] S. Lany and A. Zunger, *J. Appl. Phys.* **100**, 113725 (2006).
- [33] G. Makov and M. C. Payne, *Phys. Rev. B* **51**, 4014 (1995).
- [34] M. Leslie and M. J. Gillan, *J. Phys. C* **18**, 973 (1985).
- [35] S. Lany and A. Zunger, *Phys. Rev. B* **78**, 235104 (2008).
- [36] F. Oba, A. Togo, I. Tanaka, J. Paier, and G. Kresse, *Phys. Rev. B* **77**, 245202 (2008).
- [37] M. Zinkevich and F. Aldinger, *J. Am. Ceram. Soc.* **87**, 683 (2004).
- [38] M. A. Reshchikov, H. Morkoç, S. S. Park, and K. Y. Lee, *Mater. Res. Soc. Symp. Proc.* **693**, 365 (2002).
- [39] M. A. Reshchikov and R. Y. Korotkov, *Phys. Rev. B* **64**, 115205 (2001).